Sustainable Chemical Engineering
https://ojs.wiserpub.com/index.php/SCE/

UNIVERSAL WISER PUBLISHER

Research Article

Effect of Substrate on Active Material and Dynamic Performance Enhancement in Supercapacitor Devices Based on Graphite-Clay Composite Electrodes

Pannilage M. H. Madhushanka[1], R. K. D. A. Neranjani[2], Kohobhange S. P. Karunadasa[3*], Chinthan H. Manoratne[3]

[1]Postgraduate Institute of Science, University of Peradeniya, Peradeniya, 20400, Sri Lanka
[2]Department of Nano Science Technology, Faculty of Technology, Wayamba University of Sri Lanka, Kuliyapitiya, 60200, Sri Lanka
[3]Materials Technology Section, Industrial Technology Institute, No. 363, Baudhdhaloka Mawatha, Colombo 07, 00700, Sri Lanka
E-mail: sujithkohobhange@yahoo.com

Received: 11 August 2025; **Revised:** 16 October 2025; **Accepted:** 27 October 2025

Abstract: Graphite-clay composite electrodes are promising candidates for fabricating energy storage devices with Polyaniline (PANI) as the active material. Well-performing homogeneous symmetric supercapacitors made from graphite-clay electrodes open a new pathway to construct heterogeneous symmetric supercapacitors, providing a novel technological perspective on supercapacitors. The present study demonstrates the fabrication of three different supercapacitors, including a PANI-coated graphite-Montmorillonite (MMT) composite electrode and graphite-kaolinite-cement composite electrode-based supercapacitor (PANI-GMMTCE_GKCeCE), a PANI-coated graphite-MMT-cement composite electrode and graphite-kaolinite-cement composite electrode-based supercapacitor (PANI-GMMTCeCE_GKCeCE), and a PANI-coated graphite-kaolinite composite electrode and graphite-kaolinite-cement composite electrode-based supercapacitor (PANI-GKCE_GKCeCE), and their performance evaluation using various electrochemical and analytical techniques. Supercapacitors were constructed based on four different PANI-coated graphite-clay composite electrodes, each consisting of PANI-GKCeCE, with the remaining section from each of the other electrodes. Each electrode surface facilitated the formation of conductive PANI coating via aniline electropolymerization, as evidenced by well-characteristic Cyclic Voltammograms (CV) with dominant peaks. The morphological structures of PANI coating on each electrode are unique from one another, but all have a PANI nanofiber network with uniform or irregular distribution. Synergistic interactions of two different PANI networks in a supercapacitor contribute to the charge transfer and storage mechanisms. Both (PANI-GMMTCE_GKCeCE) and (PANI-GMMTCeCE_GKCeCE) supercapacitors outperformed in capacitance, producing more than 390 $F \cdot g^{-1}$ of specific capacitance in CV and charge-discharge tests. All three supercapacitors follow pseudocapacitive behavior in charge-discharge as well as in CVs. However, each supercapacitor displayed combined properties of double-layer and pseudocapacitor, indicating a constant phase element in each impedance spectrum. The ionic diffusion process contributed to the charge transport and storage mechanism due to the heterogeneous nature on both sides, which is similar to previously fabricated PANI-coated graphite-clay-based supercapacitors. Charge-discharge curves of each supercapacitor exhibited cyclic stability with higher Coulombic efficiency, and all supercapacitors achieved considerably higher energy and power densities, indicating the high performance of heterogeneous symmetric graphite-clay-based supercapacitors. Further modifications of heterogeneous symmetric supercapacitors are essential to improve their performance for commercial-scale development.

Copyright ©2025 Kohobhange S. P. Karunadasa, et al.
DOI: https://doi.org/10.37256/sce.7120268219
This is an open-access article distributed under a CC BY license
(Creative Commons Attribution 4.0 International License)
https://creativecommons.org/licenses/by/4.0/

Keywords: heterogeneous symmetric supercapacitor, PANI-coated graphite-clay composite electrodes, electropolymerization, coulombic efficiency

1. Introduction

Supercapacitors are one of the most promising energy storage devices for the future's vital energy demands. Supercapacitors, also known as electrochemical capacitors, can be classified into three types. An electrochemical double-layer capacitor stores energy through the ionic charge separation or adsorption of ions at the electrode-electrolyte interface.[1-3] The second one, a pseudo or redox capacitor, stores energy due to the redox reactions that take place in the active electrode materials at characteristic potentials.[2,3] The third type is a battery-like capacitor, which follows an energy storage process similar to a battery.[1] These capacitors are gaining attention due to their impressive characteristics, including superior specific capacitance, rapid charge-discharge, long lifespan, low cost, high power density, and environmental safety.[2,4] These unique features have contributed to their utilization in various electronic and electrical appliances in the recent decade. Scientists are working on enhancements and modifications to develop a more advanced version of supercapacitors that exhibits improved performance. Based on evidence supported by literature, performance enhancement can be achieved through the fabrication process, including optimizing electrodes, active materials, and electrolytes that directly contribute to the performance of a supercapacitor.[5-7] Each compartment of a supercapacitor plays a key role in facilitating charge transfer and storage, thereby significantly impacting its overall performance.

The electrode serves as the substrate for the active electrode material and forms the base of the supercapacitor; it is one of the most critical components that influence the supercapacitor's performance. The composition and nature of the electrode are vital parameters that determine its effectiveness. Graphite is one of the widely used materials in electrode fabrication due to its low cost, excellent conductivity, chemical inertness, and ease of fabrication.[8,9] The authors previously fabricated electrodes using graphite mixed with clay as a binding agent, defined as graphite-clay composite electrodes, and the further incorporation of cement reinforces the mechanical strength.[10-13] Those electrodes demonstrated significant properties, including excellent electrical conductivity and mechanical strength,[10-13] and were capable of being used in energy storage device fabrication.[12,14,15] In addition, the nature of the electrode influences the characteristics of the active electrode material, such as conducting polymers utilized in fabricating supercapacitors. For example, the authors described different morphological arrangements of Polyaniline (PANI) observed on several graphite-clay composite electrode surfaces in previous studies, proving the dependency of electrode composition on the featured polymer characteristics.[10-13] Several types of graphite-clay composite electrodes were utilized to produce PANI, and a unique PANI nanofiber network was observed on each electrode surface.[11-17] PANI nanofibers are the most conductive form of PANI and are useful to fabricate high-performance supercapacitors.[18] Building on the advantages gained from graphite-clay composite electrodes, supercapacitors constructed with two identical PANI-coated electrode segments demonstrated excellent performance, including high capacitance, greater coulombic efficiency, and favorable electrochemical properties as reported in previous studies.[12,14,15] Homogeneous supercapacitors were constructed using Graphite-MMT (GMMTCE), Graphite-MMT-cement (GMMTCeCE), Graphite-kaolinite (GKCE), and Graphite-Kaolinite-Cement (GKCeCE) composite electrodes, and each produced a PANI coating on the electrode's surface. Among them, GMMTCeCE exhibited a multi-layered PANI network with higher specific capacitance (1,002 $F \cdot g^{-1}$),[12] while others displayed considerably higher capacitance, including GKCeCE (482 $F \cdot g^{-1}$),[14] GKCE (416 $F \cdot g^{-1}$),[14] and GMMTCE (342 $F \cdot g^{-1}$),[15] accompanied by well-distributed PANI networks.

Utilizing the advantages of graphite-clay composite electrodes and their applicability in energy storage devices, this study demonstrates the fabrication of supercapacitors using non-identical PANI-coated graphite-clay composite electrode segments. Three non-identical heterogeneous symmetric supercapacitors were constructed using the previously described fabrication process, and their performance was evaluated comparatively through specific capacitance, electrochemical impedance, and charge-discharge performance. Since the graphite-clay composite electrode surfaces provide an excellent substrate for obtaining diverse PANI morphologies with varying sizes, widths, and distributions, supercapacitors fabricated from these electrodes offer significant potential for performance enhancement. Furthermore, heterogeneous symmetric supercapacitor fabrication represents a novel approach in supercapacitor technology,

presenting the combination of non-identical polymer morphologies to enhance device performance. Additionally, this approach enables the investigation of how distinct polymer properties affect electrochemical impedance, charge transfer, and storage characteristics of supercapacitors. Therefore, the outcomes of heterogeneous symmetric supercapacitors open new avenues for supercapacitor fabrication using PANI-coated graphite-clay composite electrodes.

2. Experimental

2.1 *Materials*

Natural graphite, the major conductive raw material (> 99.9%, average particle size 39.1 μm), was obtained from Bogala Graphite Lanka PLC, Sri Lanka. The secondary raw materials, including MMT (> 99%, average particle size 4.5 μm), kaolinite (> 98%, average particle size 1.2 μm), and cement (> 98%, average particle size 1.5 μm) were supplied by the Department of Geology, University of Peradeniya, Sri Lanka. H_2SO_4 (98%) and HCl (> 37%) were procured from Sigma-Aldrich Ltd, USA. Aniline (> 99.5%) was provided by Honeywell Riedel-de Haen, Germany, and used in doubly-distilled form. It was stored in a dark container in an oxygen-free environment before use.

2.2 *Fabrication of electrodes*

Four types of electrodes were fabricated according to the standard methodology introduced in the initial graphite-clay electrodes process, with changing process parameters and conditions to enhance the fabrication process.[10,11,13] Two binary electrodes, GMMTCE and GKCE, were fabricated by mixing graphite with MMT and kaolinite, respectively, at a 4 : 1 weight ratio, respectively.[10,11] On the other hand, graphite, MMT, and graphite, kaolinite with cement were mixed at a 16 : 3 : 1 weight ratio to fabricate GMMTCeCE and GKCeCE, respectively.[12,13] Each composite was prepared using deionized water, followed by continuous stirring for 2 hours at 360 rpm using an overhead stirrer (IKA Labortechnik, Germany). The dried composite was achieved by drying the composite slurry at 120 ℃ for 48 hours in a laboratory oven (Menmert, Germany). The dried powder (5.0 g each) obtained after crushing the composite was placed in a stainless-steel mold and pressed under the ram force of 2.2×10^4 N for 30 min using a manual hydraulic press (CARVER 3853-0, USA). The preform electrode was heated at 550 ℃ for 30 min in a programmable high-temperature furnace (Nabertherm, Germany). The prepared electrodes (length-3 cm and diameter-1 cm) were connected to a Cu current collector (> 99% purity, Ø 1.0 mm) from the top surface and modified with insulating paint (Nippon, Japan) to reduce the active surface area.

2.3 *Electropolymerization of aniline on electrodes*

Aniline was electropolymerized on the active electrode surfaces to produce Polyaniline (PANI), which was then used in the fabrication of supercapacitors. PANI coatings were obtained by 50 consecutive cycles of Cyclic Voltammetry (CV) using a three-electrode system in a 50 mM aniline solution with 1 M HCl as the background electrolyte. Cyclic voltammograms were acquired within a voltage window of -0.5 V to 1.2 V at 25 $mV \cdot s^{-1}$ for all electrodes, except GKCE, which was executed from -0.5 V to 1.3 V. The three-electrode system consisted of the reference electrode [Ag/AgCl electrode, ALS Co. Ltd, Japan, E = + 0.205 V vs standard hydrogen electrode], platinum wire as the counter electrode (Pt wire, ALS Co. Ltd, Japan), and the working electrode of interest. The aniline solution was degassed with high-purity, oxygen-free nitrogen gas for 30 min before each polymerization process. The morphological arrangement of PANI on each electrode surface was observed using a Scanning Electron Microscope (SEM, ZEISS EVO LS15, Germany) with a magnification of (× 50,000) at a tube voltage of 20 kV.

2.4 *Fabrication of energy-storage devices (supercapacitor)*

Three types of supercapacitor cells, including PANI-(GMMTCE_GKCeCE), PANI-(GMMTCeCE_GKCeCE), and PANI-(GKCE_GKCeCE), were fabricated using four different PANI-coated electrodes. Each supercapacitor device was constructed by sandwiching two non-identical (heterogeneous symmetric) PANI-coated electrodes (Ø-1.0 cm, area-7.86×10^{-5} m^2) with filter paper (Whatman, 41, ashless, Ø-1.0 cm, area-7.86×10^{-5} m^2) soaked in 1 M H_2SO_4 (as

the electrolyte) placed between two electrodes (Figure 1).[15] A thin layer of PANI coating was observed on the bottom surface of each electrode after 50 consecutive cycles of CV. The specific capacitance of each supercapacitor cell was determined by solid-state CV carried out from -1.5 V to 1.5 V at the scan rates of 5 $mV \cdot s^{-1}$, 15 $mV \cdot s^{-1}$, and 25 $mV \cdot s^{-1}$. The specific capacitance of each supercapacitor was calculated at each scan rate by equation (1).[15]

$$C_S = \frac{\int_{V_a}^{V_C} I_V dV}{mv(V_C - V_a)}. \quad (1)$$

Where C_S, m, v, and (V_C-V_a) are specific capacitance ($F \cdot g^{-1}$), the mass of active material (g), scan rate ($mV \cdot s^{-1}$), and potential window (V), respectively. The area under the voltammogram curve ($I_V dV$) was calculated by integrating corresponding CV curves. The electrochemical properties of each supercapacitor cell were determined by Electrochemical Impedance Spectroscopy (EIS) from 100 kHz to 10 mHz. The performance of each supercapacitor cell was evaluated using Galvanostatic Charge-discharge with Potential Limitation (GCPL) technique, conducted within -1 V to 1 V at 1 mA up to 50 charge-discharge cycles. The average specific capacitance of each supercapacitor cell was determined based on equation (2).[19]

$$C_S = \frac{I \times \Delta t}{m \times \Delta V}. \quad (2)$$

Where C_S is specific capacitance, I is the discharge current, Δt is the discharge time, ΔV is the potential window, and m is the mass of active material (PANI), respectively. The mass of active material was measured after experimental analysis of each supercapacitor, carefully removing PANI from both electrodes and then drying it. The Coulombic efficiency of each supercapacitor's charge-discharge cycles was determined using the following equation (3).[20]

$$\eta = (t_d/t_C) \times 100\%. \quad (3)$$

Where η is Coulombic Efficiency, t_d is the discharge time, and t_c is the charging time, respectively. The energy density and power density are significant parameters used to evaluate the performance of supercapacitors. The following equations were used to calculate those parameters related to the supercapacitor device.[19]

$$E = \frac{1}{2} C_{cell} V^2. \quad (4)$$

$$P = \frac{E}{\Delta t}. \quad (5)$$

Where the energy density, specific capacitance, cell potential, power density, and discharge time are denoted as E, C_{cell}, V, P, and Δt, respectively.

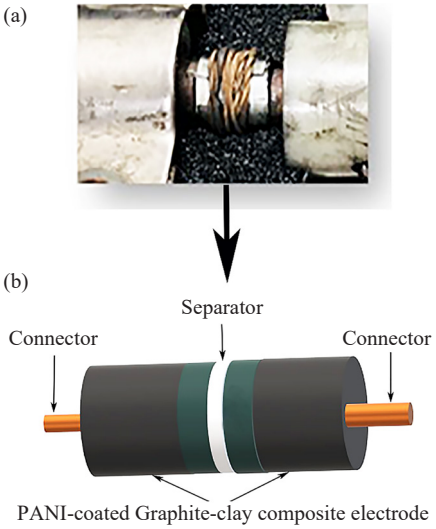

Figure 1. (a) Supercapacitor device fabricated by PANI-coated electrodes; (b) Schematic diagram of the supercapacitor device consisted of two PANI-coated electrodes and a separator

3. Results and discussion

3.1 *Electropolymerization of aniline on different electrodes*

Polyaniline (PANI) is produced by electropolymerizing aniline on different electrode surfaces to fabricate supercapacitors. It is considered one of the most promising organic conductive polymers due to its notable characteristic features, including greater conductivity, environmental stability, ability to undergo various oxidation and reduction forms, redox reversibility, and ease of preparation in aqueous media.[3,12,21,22] Among these properties of PANI, chemical stability and conductivity are vital for the fabrication and performance of supercapacitors. Excellent chemical stability of PANI is attained due to its structural formation involving a nitrogen-based salt rather than a highly reactive carbonium ion; the conductivity of PANI depends on the degree of oxidation and the degree of protonation of the material.[23] The electropolymerization process successfully achieved PANI coatings on each electrode, utilizing 50 consecutive cycles of CVs. While each voltammogram displayed slight variations from one another, they were similar to previously fabricated graphite-clay composite electrodes. Because the electrochemical oxidation of aniline to produce PANI depends on the electrode material, it is expected to observe these variations in peak potentials and currents. Because the surfaces of graphite-clay composite electrodes facilitate the detection and polymerization of aniline, well-dispersed, characteristic voltammograms are obtained, leading to a supportive pathway for producing unique PANI. Notably, each voltammogram showed three prominent peaks with slightly varied peak potentials and currents corresponding to three distinguishable oxidation states of PANI (Table 1 and Figure 2).[10-13,16,17] Peaks 1 and 2 correspond to the oxidation process, in which the former is associated with the formation of emeraldine, a half-oxidation state, and the latter is related to the fully-oxidized state, pernigraniline formation.[23] Leucoemeraldine, the fully-reduced form of PANI, is represented by peak 3 in CVs; it appears as broad peaks in all voltammograms, often accompanied by one or two minor peaks.[23]

Aniline electropolymerization is a cyclic process that occurs in multiple stages. Each stage represents a unique molecular structure of PANI and is vital for completing polymerization.[24] However, the final product of PANI consists of a mixture of different oxidation states, and its properties depend on the composition of each type.[23,24] For supercapacitor fabrication, it is essential to produce the emeraldine form, which contributes more to conductivity than the other oxidative forms of PANI. Based on the molecular structure of emeraldine, it displays the highest conductivity because of extensive π-conjugation in the PANI chain, along with four identical resonance structures. In all resonance forms, all N atoms bear a + 0.5 charge, and the C-N bonds are identical, intermediate between a single and a double bond. Furthermore, C_6H_4 rings are identical in each structure, and they consist of intermediates of benzenoid and quinoid rings. These resonance contributions form a highly conjugated π system, leading to higher conductivity in emeraldine form by imparting extra stability compared to other PANI forms.[23] According to the peaks in voltammograms, in

peak 1, all electrodes showed higher peak currents, except GKCeCE, which showed a comparatively lower peak current. Although peak currents are high, they are not the sole factor influencing the production of a higher amount of conductive PANI, since the conversion from emeraldine to pernigraniline and leucoemeraldine by oxidation and reduction, respectively, is also crucial for the final conductivity of PANI.[17,18] The amount of conversion is affected by the currents of peaks 2 and 3; sometimes, those higher currents in peak 2 are responsible for overoxidation that reduces the amount of conductive PANI.[18] Therefore, these peak currents are good indications of producing conductive PANI, but they are not the only factor determining it. Overall, each electrode produces a sufficient amount of emeraldine form of PANI, which can be utilized in the fabrication of supercapacitors.

Table 1. Average peak potential and peak current of cyclic voltammograms related to the electropolymerization of aniline on different electrode surfaces

Type of electrode	E (V)			$I \times 10^{-3}$ (A)		
	Peak 1	Peak 2	Peak 3	Peak 1	Peak 2	Peak 3
GMMTCE	0.335	0.753	0.364	21.381	24.525	24.641
GMMTCeCE	0.348	0.684	0.404	20.294	14.649	20.572
GKCE	0.405	0.61	0.378	20.408	13.731	15.842
GKCeCE	0.29	0.728	0.315	6.895	10.632	13.923

E-Average peak potential, *I*-Average peak current

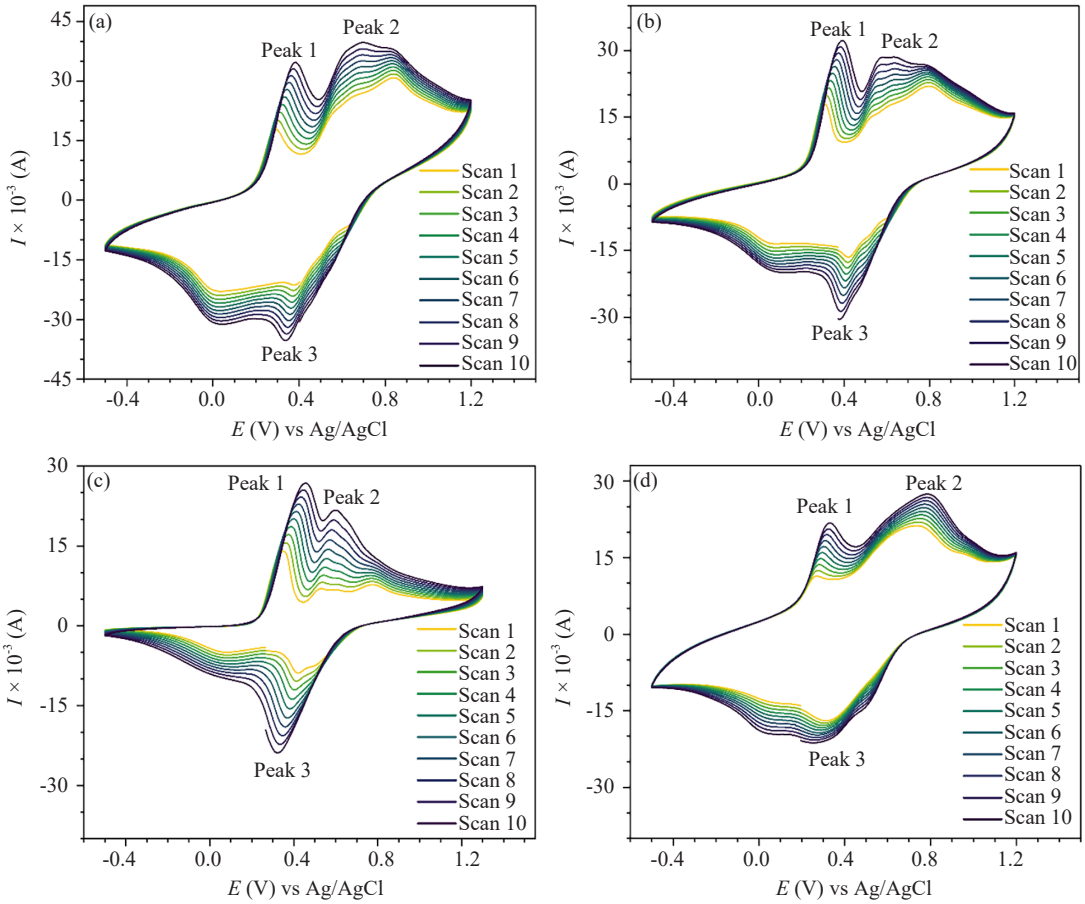

Figure 2. Cyclic voltammograms with ten consecutive cycles obtained via electropolymerization of PANI on four electrodes: (a) GMMTCE; (b) GMMTCeCE; (c) GKCE; (d) GKCeCE

PANI morphology is another factor that affects the conductivity.[25] Several morphological structures of PANI, including nanowires, nanorods, nanofibers, nanospheres, and nanotubes, are well-reported in the literature with their characteristic applications.[26-28] Due to the remarkable properties of PANI nanofibers, such as high effective surface area, interlinked porous network, ease of contact with each other, and ability to form dense networks, they are utilized as a precise material for charge storage in supercapacitors.[3,26,29] The morphological variations of PANI affect the conductivity of the whole system, controlling electrochemical performance, which depends on the shape of PANI when its dimension are diminished to the nanoscale.[26] The morphological structure of each electrode was observed under SEM, showing comparatively similar structures on each electrode with slightly varied sizes and distributions (see Figure 3). PANI-GMMTCE consists of a densely-packed PANI nanofiber network with relatively small pores between fibers, while PANI-GMMTCeCE counterpart shows a well-distributed multi-layered PANI nanofiber network, especially with thinner nanofibers. Considering the remaining structures, there is a uniformly distributed PANI nanofiber network on PANI-GKCE with wider pores; in contrast, PANI-GKCeCE exhibits densely packed PANI nanofibers with fine pores. Overall, every electrode has been shown to produce a PANI nanofiber network, which is similar to previously fabricated graphite-clay composite electrodes, proving their capabilities in energy storage applications.[11-13,15,16]

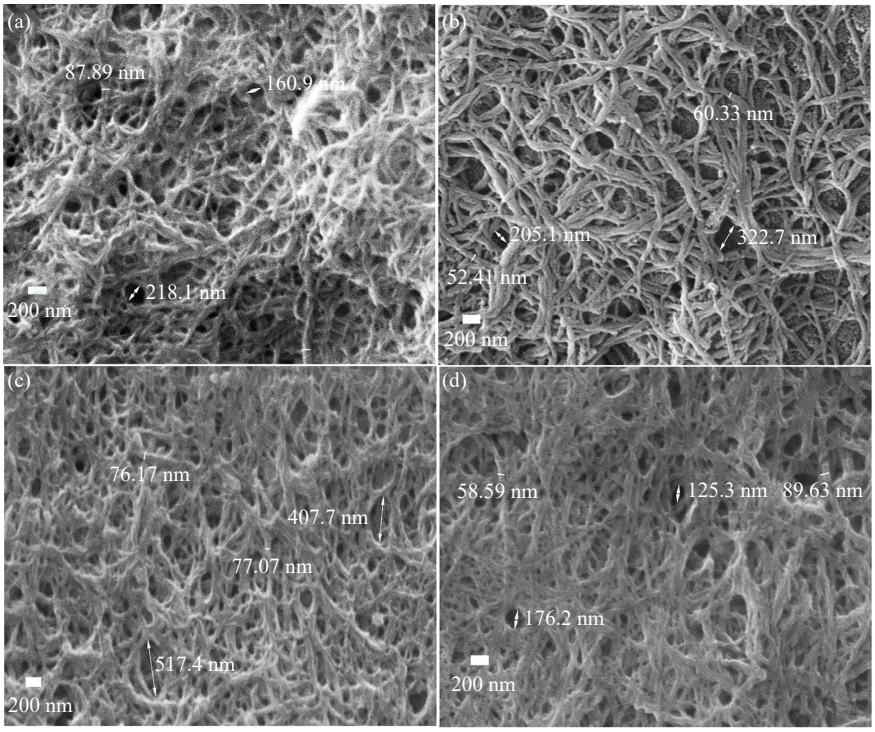

Figure 3. Morphological Strucutres of PANI nanofibers obtained on each electrode observed using SEM under the magnification of (× 50,000): (a) PANI-GMMTCE; (b) PANI-GMMTCeCE; (c) PANI-GKCE; (d) PANI-GKCeCE

However, the variations in the size of nanofibers and the width of nanopores can significantly contribute to the outcomes of capacitive and electrochemical properties of supercapacitors. The presence of a fiber network in the nanometer range is advantageous for energy storage devices because it allows for the formation of an interconnection of fibers by increasing the conductivity of the polymer layer. Additionally, a well-distributed porous nanofiber network facilitates ion transport and diffusion between polymer layers, leading to effective charge transfer and storage mechanism in supercapacitors.

According to the morphological characteristics of previously fabricated graphite-clay composite electrodes, the Graphite-Colloidal Graphite-Kaolinite-Cement Composite Electrode (GCGKCeCE) based homogeneous supercapacitor displayed the highest specific capacitance among all electrodes, due to the presence of PANI nanofiber network with villi-like formations.[17] This improves the conductivity of PANI and forms strong interactions between PANI and the

electrode surface, as proven by the lowest R_S and R_{CT} values.[17] Multi-layered PANI nanofiber network in GMMTCeCE contributes to higher specific capacitance of its homogeneous symmetric supercapacitor, while its heterogeneous counterpart displayed the highest value among the three of these heterogeneous symmetric supercapacitors.[12] On the other hand, the appearance of PANI nanofiber network without specific features in GMMTCE, GKCE, and GKCeCE showed comparatively lower specific capacitance of their homogeneous and heterogeneous counterparts due to moderate charge transfer and storage capabilities of PANI.

Conclusively, PANI produced by electropolymerization provides a pathway to develop effective heterogeneous symmetric supercapacitors from graphite-clay composite electrodes through the formation of highly conductive PANI nanofiber networks on each electrode surface.

3.2 *Fabrication of supercapacitor devices*

Supercapacitors are among the most impactful energy storage devices, offering an effective solution for meeting future energy demands. Graphite-clay composite electrodes have recently been utilized in the fabrication of supercapacitors using conductive polymers, such as PANI, due to their electrochemical and energy storage properties.[12,14-17] A supercapacitor is composed of two electrode segments that act as blocking electrodes, active materials such as conductive polymers, which serve as the active components for charge transfer and storage, and a separator containing an electrolyte that forms an ionic bridge between the two electrodes.[2]

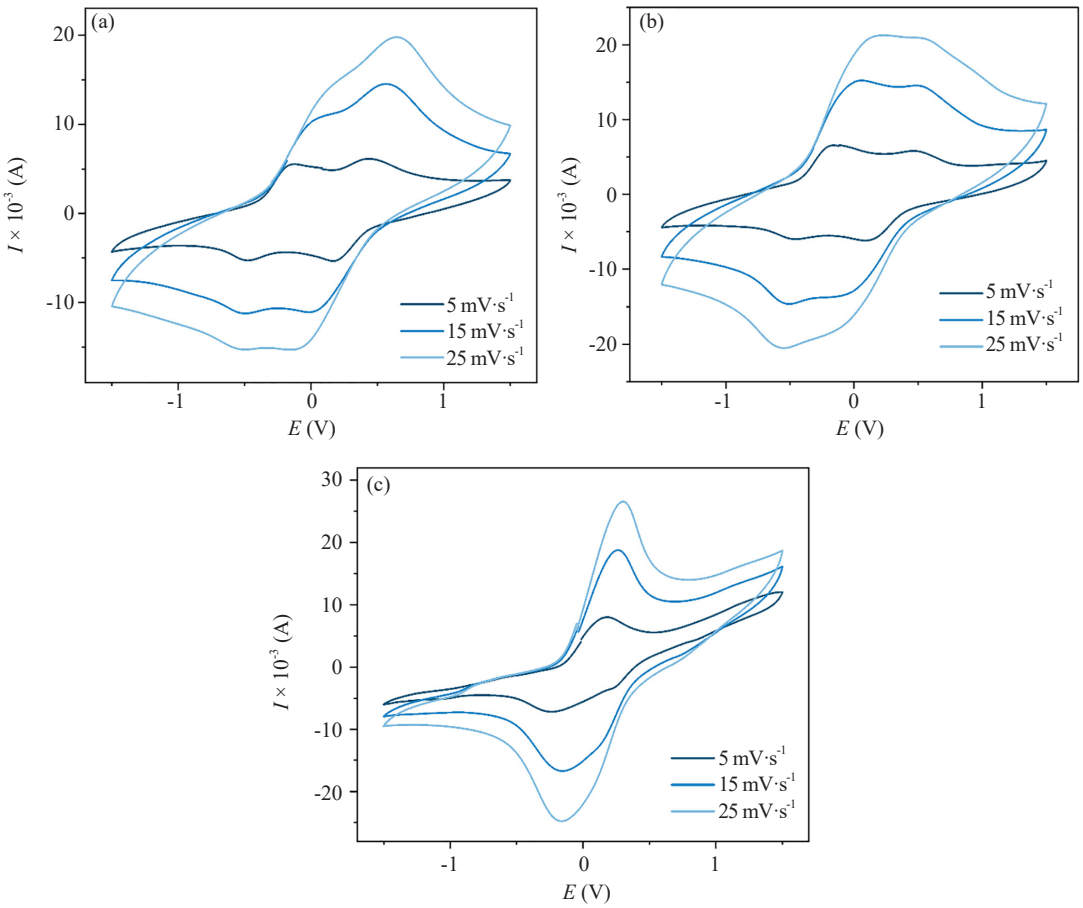

Figure 4. Solid-state CVs of each supercapacitor cell with varying scan rates: (a) PANI-(GMMTCE_GKCeCE); (b) PANI-(GMMTCeCE_GKCeCE); (c) PANI-(GKCE_GKCeCE)

Three heterogeneous symmetric supercapacitors were fabricated and their capacitive performance was evaluated

through solid-state CVs (Figure 4). According to the literature, a square shape appears in the double-layer capacitor, while the presence of redox peaks in square-shaped CV indicates pseudocapacitive nature.[3,15] Based on shapes depicted by voltammograms, all CVs display two or more redox peaks, proving the absence of pure double-layer capacitive characteristics in heterogeneous symmetric supercapacitors. All three supercapacitors displayed redox peaks in deviated square-shaped CVs, showcasing their relations to pseudocapacitive nature.[1]

When the scan rate is increased, the peaks become wider than the former ones, and the specific capacitance decreases due to the time limit for ion diffusion between the active pore sites of PANI and the external surface of the electrolyte in the supercapacitor. The variations in specific capacitance when increasing scan rates follow a slightly polynomial decrease in each supercapacitor (see Figure 5). Since PANI morphologies are not identical to each other, the ion accumulation and diffusion vary on both sides of the supercapacitor. However, all supercapacitors showed at least one broad peak at higher rates, indicating the consistency of their initial capacitive features at high scan rates. On the other hand, the disappearance of peaks observed at higher rates in previously fabricated supercapacitors using homogeneous graphite-clay electrodes, reflects the conversion from pseudo-capacitance to the double-layer type at higher rates. Thus, the construction of supercapacitors using heterogeneous symmetric PANI-coated electrodes is beneficial for achieving similar capacitive properties at higher scan rates.

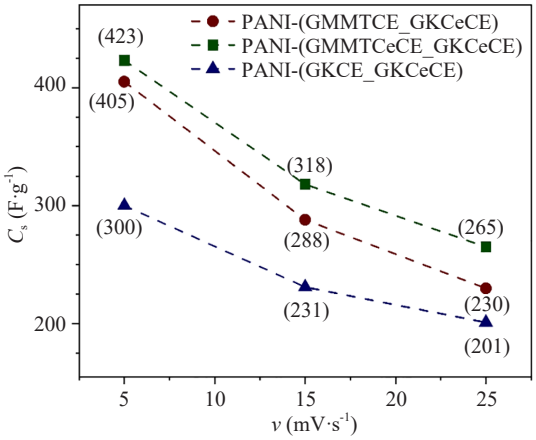

Figure 5. The variation of specific capacitance of each supercapacitor cell at different scan rates: (a) PANI-(GMMTCE_GKCeCE); (b) PANI-(GMMTCeCE_GKCeCE); (c) PANI-(GKCE_GKCeCE)

PANI structural heterogeneity in both sides of each supercapacitor device contributed to displaying specific characteristic features compared to homogeneous supercapacitor devices. Considering each device, the PANI-GKCeCE compartment is common for all, but the other compartment varies for each device. Therefore, final performance depends on interactions between both sides. PANI-GKCeCE, the common compartment of each supercapacitor, consists of nanofibers that are distributed and packed with each other, forming an interfibrillar network with narrow pores, which facilitates efficient electrolyte ion accumulation and diffusion. PANI-(GMMTCeCE_GKCeCE) displayed the highest specific capacitance (C_S) (423 F·g^{-1}) among all three heterogeneous symmetric supercapacitors based on CV, while PANI-(GMMTCE_GKCeCE) is closer C_S to the former one (405 F·g^{-1}), and the lowest C_S is 300 F·g^{-1} for PANI-(GKCE_GKCeCE). Based on the literature, PANI-based homogeneous supercapacitors, which were made from GMMTCE (342 F·g^{-1}),[15] GKCE (416 F·g^{-1}),[14] GKCeCE (482 F·g^{-1}),[14] showed closer values of C_S to heterogeneous symmetric supercapacitors. In addition to those PANI-based graphite-clay composite electrodes, C_S values are comparatively higher than those of supercapacitors fabricated by various PANI morphological structures, including PANI aerogels (184 F·g^{-1}),[30] PANI nanofibers (252 F·g^{-1}),[31] and PANI nanorods (297 F·g^{-1}).[32] These results demonstrated that heterogeneous symmetric supercapacitors are capable of obtaining comparatively higher C_S.

Electrochemical Impedance Spectroscopy (EIS) is used to determine the electrochemical properties of each heterogeneous symmetric supercapacitor and to explore the diversity of new features of electrochemical impedance in heterogeneous symmetric PANI-coated energy storage devices. Nyquist plots related to each supercapacitor with equivalent circuits are in Figure 6. Each Nyquist plot displays a unique-shaped spectrum with the appearance of different elements in those equivalent circuit models, confirmed by the existing literature.[33-36] Each EIS spectrum exhibits a deviated semi-circular arc in the high frequency region and continues it as a straight or angular line with an angle between 30° and 75°.

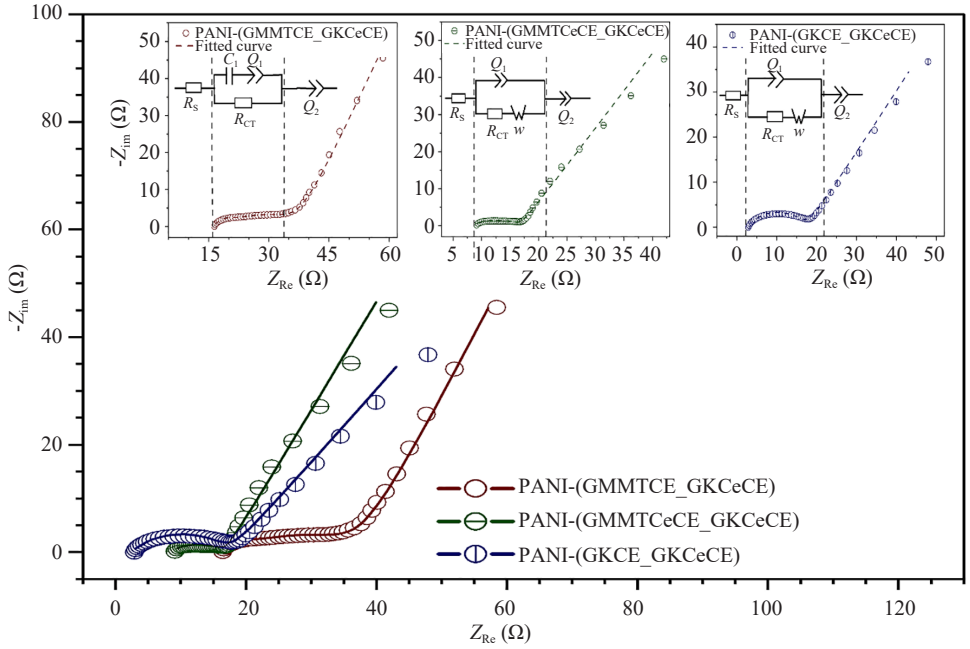

Figure 6. Nyquist plots of each supercapacitor cell (Inset displays (a) PANI-(GMMTCE_GKCeCE); (b) PANI-(GMMTCeCE_GKCeCE); (c) PANI-(GKCE_GKCeCE) with their corresponding equivalent circuits)

PANI-(GMMTCeCE_GKCeCE) and PANI-(GKCE_GKCeCE) show identical equivalent spectra, while PANI-(GMMTCE_GKCeCE) is different from those spectra. Although similar spectra appear, the values of each element in each circuit vary (See Table 2). Each spectrum's starting point is related to the serial Resistance (R_S) associated with the electrode and PANI coating, which depends on the structural stability forming the interactions between PANI and the electrode of each supercapacitor. It indicates the conductivity of PANI nanofibers in each supercapacitor, which means lower R_S indicates higher electronic conductivity of PANI, corresponding to a higher abundance of emeraldine forms.[37] When PANI-electrode interactions become strong, lower R_S can be observed. According to the Nyquist plots of each supercapacitor, R_S varies as follows: R_S (PANI-GKCE_GKCeCE) < R_S (PANI-GMMTCeCE_GKCeCE) < R_S (PANI-GMMTCE_GKCeCE). This variation indicates how PANI binds with the graphite-clay composite electrode surface, forming effective interactions with both faces. The lowest R_S in PANI-GKCE_GKCeCE suggests that both GKCE and GKCeCE electrode surfaces make strong interactions with PANI through π electrons between graphite sheets and PANI nuclei compared to the other two counterparts. Densely packed nanofibers in both GKCE and GKCeCE make proper interconnection with those electrode surfaces; conversely, GMMTCE and GMMTCeCE nanofiber networks develop comparatively stable PANI-electrode systems that are effective for low R_S. Because these supercapacitors consisted of heterogeneous symmetric PANI-electrode systems on both sides, the combined effect of structural stability in each supercapacitor gives rise to the formation of strong interaction with lower R_S values. However, randomly distributed PANI nanofiber clusters in PANI-GMMTCE caused an increase in R_S; by contrast, the multilayered PANI nanofiber network in PANI-GMMTCeCE contributed to a moderate R_S value compared with each other. Furthermore, PANI in GKCE and GKCeCE combination contains the highest amount of emeraldine form than

the other two electrodes. The composition of emeraldine in electrodes varies according to the following order: PANI-GMMTCE < PANI-GMMTCeCE < PANI-GKCE, and it can be displayed with a sharp peak 1 in each spectrum of CVs in electropolymerization (Figure 2). Therefore, both the conductivity of PANI and the strength of interactions between PANI and the electrode surface significantly affect R_S values.

Table 2. Fitted values of each equivalent circuit model for EIS spectra of three supercapacitors

Element	Supercapacitor		
	PANI-(GMMTCE_GKCeCE)	PANI-(GMMTCeCE_GKCeCE)	PANI-(GKCE_GKCeCE)
R_S/Ω	14.46	8.22	2.45
R_{CT}/Ω	22.49	8.72	14.97
C_1/F	3.23×10^{-3}	-	-
Q_1/F·s$^{(\alpha-1)}$	5.27×10^{-3}	3.08×10^{-3}	9.35×10^{-4}
a_1	0.321	0.395	0.524
Q_2/F·s$^{(\alpha-1)}$	1.52×10^{-1}	2.25×10^{-1}	7.92×10^{-1}
a_2	0.730	0.815	0.860

R_S, R_{CT}-Resistors, C_1-Capacitor, Q_1 and Q_2-Constant phase elements, a_1 and a_2-numerical values related with each constant phase element

Each Nyquist plot displayed a non-identical deviated semi-circular shaped line in the high frequency region corresponding to several elements. Capacitors with Constant Phase Element (CPE) are parallel to charge transfer resistance (R_{CT}) in PANI-(GMMTCE_GKCeCE); on the other hand, CPE is parallel to R_{CT} and is extended with a Warburg element in the other two counterparts. The deviated semicircle in all spectra indicates that it corresponds to the mixed nature of the capacitor, unlike pure capacitance. The diameter of the arc is approximately equal to the value of R_{CT}, and it represents the morphological effect of PANI.[11,36]

In morphological aspects of PANI, the higher the surface area contributes to a lower R_{CT}, resulting in a high heterogeneous electron transfer rate. R_{CT} is related to the chemical kinetics behavior of the system, and it is inversely proportional to the heterogeneous electron transfer rate constant.[11] In terms of charge transfer and storage mechanism of supercapacitor, lower R_{CT} facilitates easier accessibility of ions or charges for intercalation and deintercalation of the PANI-electrode system.[38] The variation of R_{CT} in all supercapacitors is as follows: R^{CT} (PANI-GMMTCeCE_GKCeCE) < R^{CT} (PANI-GKCE_GKCeCE) < R^{CT} (PANI-GMMTCE_GKCeCE). Considering all the factors attributed to R_{CT}, the PANI-GMMTCeCE_GKCeCE supercapacitor displays better charge transfer and storage capability supported by a highly conductive and accessible PANI nanofiber network. Due to the multi-layer PANI nanofiber network in GMMTCeCE with an interfibrillar system coordinating with PANI-GKCeCE, PANI-GMMTCeCE_GKCeCE supercapacitor shows better chemical kinetics, in terms of fast electron transfer rate, which outperforms the other two counterparts.

On the other hand, relatively higher R_{CT} values in the remaining two indicate that PANI morphological defects with cluster formation and unevenly distributed PANI network limit the efficiency of electron transfer kinetics. However, the values of R_S and R_{CT} in each supercapacitor are important indicators that are directly used to evaluate the conductivity and ionic diffusion of the supercapacitor via the solid-electrolyte interface.[39] Therefore, the variations of R_S and R_{CT} exhibit a preliminary idea of the charge transfer and storage performance in a supercapacitor, leading to the development of highly efficient energy storage devices.

In the high and mid frequency region, the presence of CPE//R_{CT} is common for all three supercapacitors, while there is a capacitor element in serial with CPE in the (PANI-GMMTCE_GKCeCE) supercapacitor. The serial combination of a capacitor and CPE in (PANI-GMMTCE_GKCeCE) produces a straight line parallel with the real impedance axis. However, the presence of CPE parallel with R_{CT} suggests similarity in the electrochemical nature of the

supercapacitor with the occurrence of PANI-GKCeCE section in each device. CPE represents a hybrid capacitive nature by combining double-layer capacitance and pseudocapacitance.

In the Nyquist plot, it can appear due to the various factors of the PANI-electrode system, including the nature of the electrode surface, porosity electrode, dynamic deviation associated with diffusion of ionic charges into the PANI-coated system, and the distribution of relaxation times as a result of inhomogeneity at the electrode-electrolyte interface.[38] Numerical parameters related to CPE are Q and a, which denote a frequency-independent constant associated with the surface and nature of the electroactive material (PANI) and a numerical variable between 0 and 1, respectively.[39] Furthermore, the variation of n value that starts from 0 is pure resistance, 1 is an ideal capacitor, and $0.5 \leq a < 1$ is moderate capacitive behavior.

The variations of Q_1 and n_1 correspond to the first CPE in each Nyquist plot of each supercapacitor as follows: Q_1 (PANI-GKCE_GKCeCE) < Q_1 (PANI-GMMTCeCE_GKCeCE) < Q_1 (PANI-GMMTCE_GKCeCE) and a_1 (PANI-GMMTCE_GKCeCE) < a_1 (PANI-GMMTCeCE_GKCeCE) < a_1 (PANI-GKCE_GKCeCE). According to these values and variations, it reflects that CPE_1 of PANI-(GKCE_GKCeCE) exhibits moderate capacitive behavior compared to the other two, also proved by less deviation of the semi-circular arc than that of the other two counterparts. However, the values of CPE_1 for all three types are closely varied from each other, showing that all CPE_1s have a closely identical nature in the capacitor.

There is a Warburg element (W) that appeared at the end of a deviated semi-circular shaped arc at the low frequency region in both PANI-(GMMTCeCE_GKCeCE) and PANI-(GKCE_GKCeCE), except PANI-(GMMTCE_GKCeCE). In electrochemical impedance, the Warburg element represents mass transport behavior, indicating ionic diffusion in electrodes and the associated system.[40] In general, W can appear individually or in combination with CPE or a capacitor, based on diffusional properties in the low-frequency region. In terms of species or ions, in solution, they diffuse toward or away from the electrode-electrolyte interface driven by a concentration gradient, which presents as Warburg impedance.[41]

Classic semi-infinite Warburg impedance behavior observed in previously fabricated PANI-coated electrode system or homogeneous supercapacitors, as well as PANI-(GMMTCeCE_GKCeCE) and PANI-(GKCE_GKCeCE) supercapacitors.[12,17] Except PANI-(GMMTCE_GKCeCE) supercapacitor, the other two counterparts displayed diffusion-controlled charge transfer process that deviates from ideal capacitive behavior. That indicates a better porosity nature in electrodes and PANI nanofiber networks, resulting strong contribution to the charge transfer process in PANI-graphite-clay supercapacitor systems. At the low-frequency range, all EIS spectra consist of a second Constant Phase Element (CPE_2), which represents the mixed capacitive properties of the supercapacitor. The variation of values of Q and a as follows: Q_2 (PANI-GMMTCE_GKCeCE) < Q_2 (PANI-GMMTCeCE_GKCeCE) < Q_2 (PANI-GKCE_GKCeCE) and a_2 (PANI-GMMTCE_GKCeCE) < a_2 (PANI-GMMTCeCE_GKCeCE) < a_2 (PANI-GKCE_GKCeCE). Variation of both values in each supercapacitor type follows the same order, and there is a disparity in the order of variation compared to CPE_1.

Conclusively, each EIS spectrum suggests that these PANI-coated graphite-clay-based supercapacitor systems exhibit behaviors closely related to battery and fuel cell circuit systems, highlighting the importance of further development.

The Bode plot is another complementary analysis to the Nyquist plot, which shows a frequency-domain representation of the electrochemical impedance of a supercapacitor. The Bode plot of each supercapacitor, displayed in Figure 7, describes the charge transfer, storage, and ion diffusion processes in each device.[42,43] The high-frequency region shows the intrinsic resistance of the supercapacitor. Bode impedance in each supercapacitor is very low, and the phase angle is close to 0°, indicating a small equivalent series resistance, which combines the resistances of electrolyte, electrode material, and PANI coatings. That ensures better conductivity and fast charge transfer rate in each supercapacitor, which has been previously proven by Nyquist plots and solid-state CVs.

In the mid-frequencyy region, phase angle variations in Bode plots are similar for both PANI-(GMMTCE_GKCeCE) and PANI-(GMMTCeCE_GKCeCE), while there is a little deviation in PANI-(GKCE_GKCeCE), indicating the influence of MMT incorporation in composites for efficient charge transfer in PANI-coated electrodes. On the other hand, there is a gradual decrease in impedance in each supercapacitor, which depicts the ion diffusion influence in each device at this transition region. In the low-frequency region, impedance increases sharply when frequency decreases in all three supercapacitors. Despite the impedance increases, the phase angle decreases up to between (-35° to -50°) in all

devices without reaching -90°, which indicates pure capacitor behavior, suggesting the non-ideal capacitor behavior. This behavior reflects the pseudocapacitive nature, similar in Nyquist plots. Therefore, each Bode plot displays characteristic features similar to the Nyquist plot in each supercapacitor, including pseudocapacitive nature, lower R_S and R_{CT} values, and influence on diffusion in the charge transfer process.

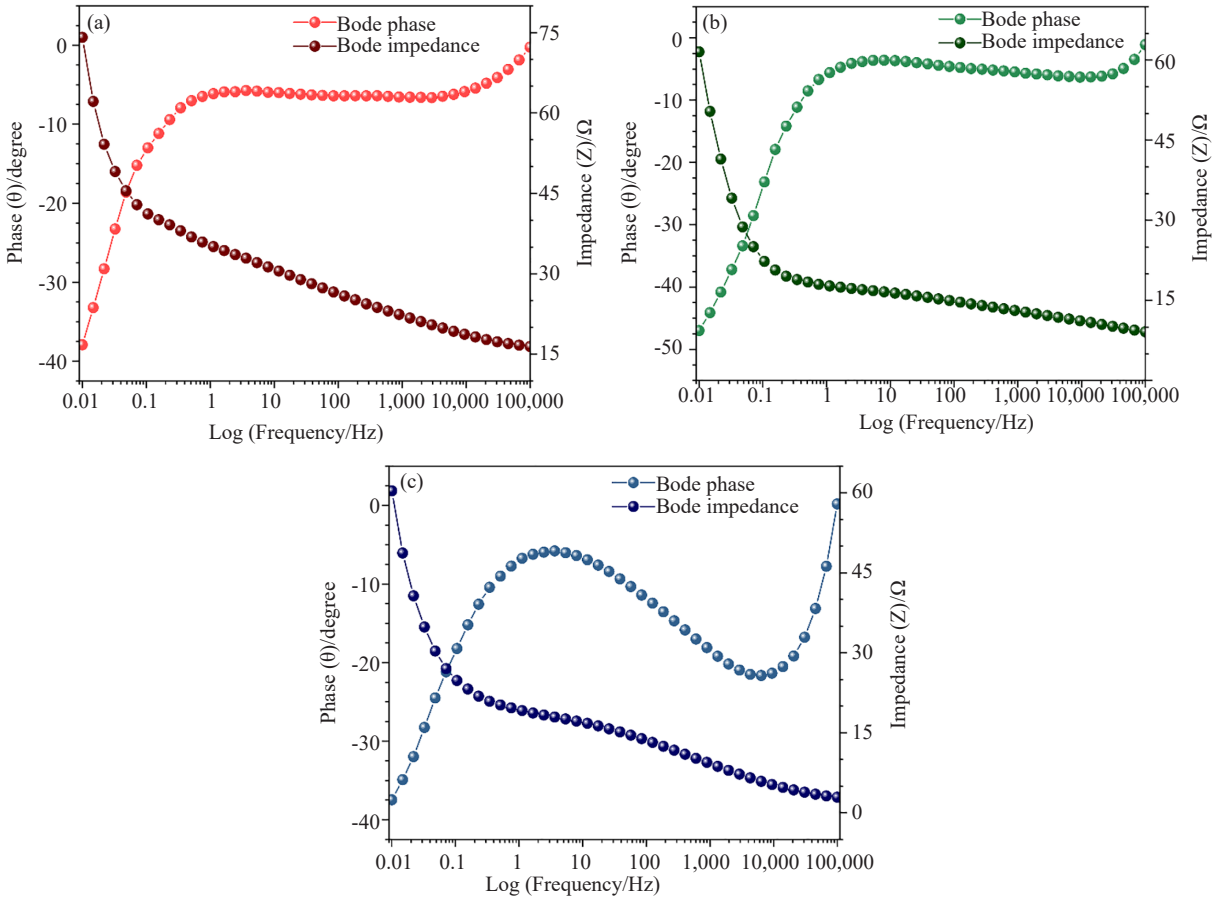

Figure 7. Bode plots related to Nyquist plot of each supercapacitor cell: (a) PANI-(GMMTCE_GKCeCE); (b) PANI-(GMMTCeCE_GKCeCE); (c) PANI-(GKCE_GKCeCE)

The Galvanostatic Charge-Discharge technique (GCD) is utilized to assess the performance of a supercapacitor in terms of cyclic stability and Coulombic efficiency. Because it exhibits the efficiency and effectiveness of charge storage mechanisms, as well as its stability, it is a useful technique for estimating supercapacitor performance.[14,17] Figure 8 shows that the initial ten charge-discharge cycles of each supercapacitor, obtained by GCD, and each GCD diagram are similar in shape, except for the first cycle. The symmetrical GCD curves in each diagram indicate high electrochemical stability and good reversibility of PANI-based heterogeneous supercapacitors.[7]

The shape of the GCD curve reflects the charge storage mechanisms, and all three supercapacitors display small disparities in GCD curves, proving there is a little significant difference in the charge storage mechanisms among them. All GCD curves are triangular without an identifiable IR drop, which is closely associated with pseudocapacitive nature, unlike batteries or double-layer characteristics.[13,16,24] The morphology of electroactive materials and the associated electrode system mainly contribute to the charge transfer and storage mechanism of a supercapacitor.

The Coulombic efficiency (η) is another parameter that is used to determine the supercapacitor performance in terms of reversibility, efficiency, and longevity. The Coulombic efficiency variation related to 50 cycles of GCD curves in each supercapacitor is displayed in Figure 9. It depicts a higher η (more than 80%) for all three supercapacitors, proving that each supercapacitor has better reversibility, longevity, and efficiency. However, each supercapacitor shows fluctuating η

values in the initial cycles, particularly during the first ten cycles. Since various-sized well-distributed pores among PANI nanofibers, PANI coatings on each electrode surface create an enhanced porous nature. In GCD, some pores remained blocked for electrolyte ions, limiting the ions from being charged or discharged in the initial few cycles.[44] This results in attaining higher/slower charging and discharging times, leading to observing very high/low η values.

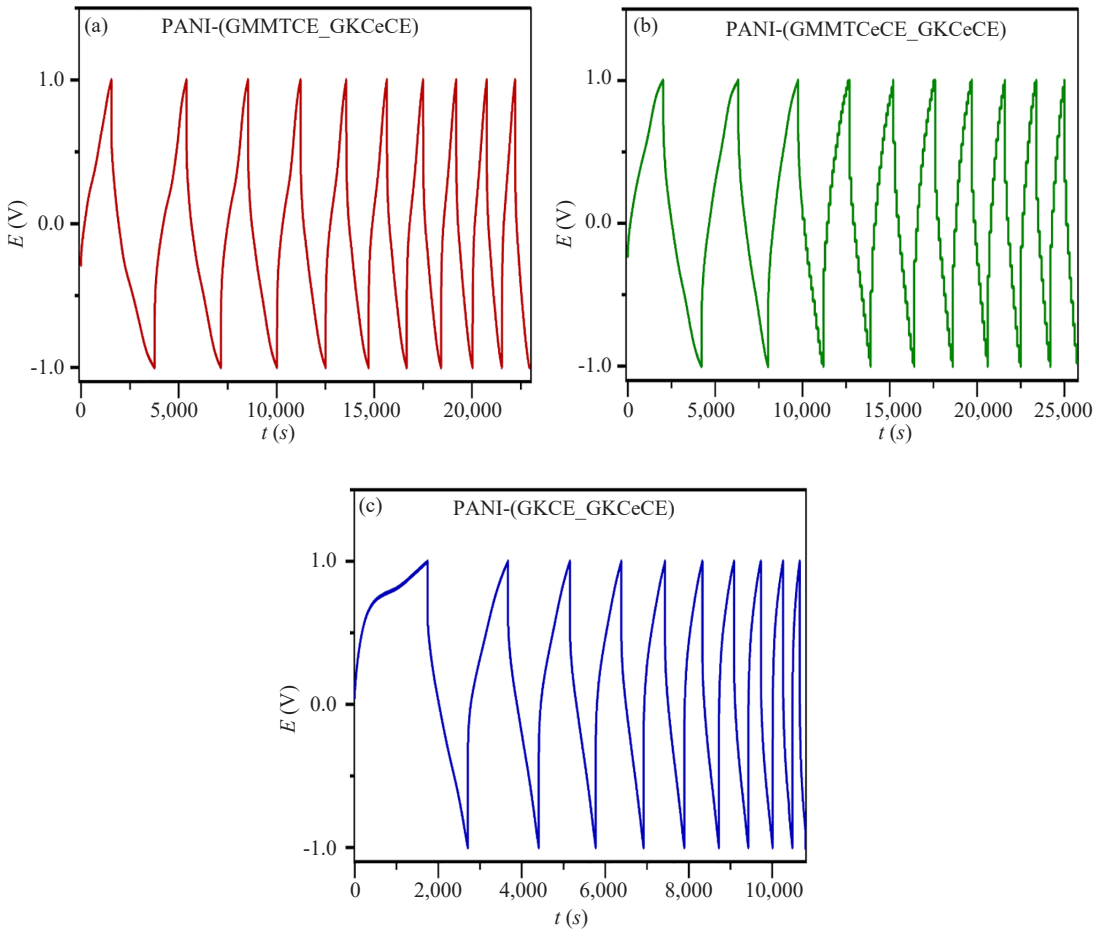

Figure 8. First ten galvanostatic charge-discharge cycles of each supercapacitor: (a) PANI-(GMMTCE_GKCeCE); (b) PANI-(GMMTCeCE_GKCeCE); (c) PANI-(GKCE_GKCeCE)

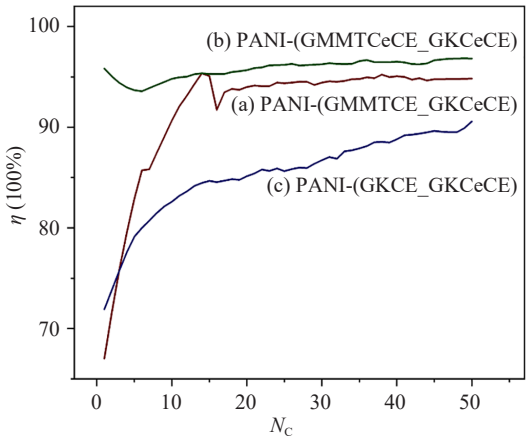

Figure 9. Coulombic Efficiency variation of each GCD curve of each supercapacitor showing upto 50 cycles: (a) PANI-(GMMTCE_GKCeCE); (b)

PANI-(GMMTCeCE_GKCeCE); (c) PANI-(GKCE_GKCeCE)

Although η values fluctuate at the beginning, after a few cycles, they are stable due to the electrolyte penetrating all pores or channels in PANI, which are accessible for charge transfer.[44] GCD curves of these heterogeneous symmetric supercapacitors followed a similar phenomenon, showing good cyclic stability that can contribute to longer lifespan.

There are major parameters, including specific Capacitance (C_S), Energy density (E), and Power density (P), are critical for evaluating a supercapacitor's performance based on GCD curves. The values of each parameter correspond to the supercapacitors listed in Table 3, clearly indicating each performance. The active electrode material has a significant impact on C_S, E, P, and the stability of each supercapacitor.

Table 3. Performance evaluation of galvanostatic charge-discharge of three supercapacitors by comparing PANI-carbon based supercapacitors

Type of supercapacitor	Specific capacitance/F·g^{-1}	Energy density/W·h·kg^{-1}	Power density/W·kg^{-1}	Reference
PANI-(GMMTCE_GKCeCE)	444	887	1,440	Present work
PANI-(GMMTCeCE_GKCeCE)	393	785	1,286	Present work
PANI-(GKCE_GKCeCE)	179	358	1,333	Present work
PANI-(GKCE_GKCE)	548	304	1,739	14
PANI-(GKCeCE_GKCeCE)	1,143	635	1,667	14
PANI-exfoliated graphite	356	318	12.5×10^3	45
PANI-graphite	238	3.0	-	46
PANI/MWCNT	277	9.8	-	47

MWCNT-Multi-Walled Carbon Nanotubes

The morphology of electroactive materials and the associated electrode system mainly contribute to the charge transfer and storage mechanism of the supercapacitor. Because PANI coatings on each electrode surface uniform or irregularly distributed, densely packed or multi-layered nanofiber networks, they create highly porous structures and an effective surface area on electrodes. These surfaces enhance the transport of electrolytic ions and improve charge transfer, enabling superior performance in a supercapacitor.[44] Following the above fact, (PANI-GMMTCE_GKCeCE) and (PANI-GMMTCeCE_GKCeCE) supercapacitors displayed higher C_S in GCD, similar to CV, compared to the (PANI-GKCE_GKCeCE) supercapacitor. In addition, both have relatively higher E values than their third counterpart, but P values are higher for all three supercapacitors. Due to the dependency of discharge time significantly on the P value, each one showed relatively identical GCD curves, resulting in a higher P.

However, the values of E and P reflect the superior performance of heterogeneous symmetric supercapacitors. Furthermore, modifications will be carried out to enhance the performance of capacitance retention, with a focus on longevity of cycling. Therefore, heterogeneous symmetric supercapacitors made from PANI-coated graphite-clay composite electrodes demonstrate excellent performanc, highlighting new directions for supercapacitor fabrication to meet future energy demands.

4. Conclusion

The present study demonstrates novel aspects of fabricating heterogeneous symmetric supercapacitors based on PANI-coated graphite-clay composite electrodes. Each voltammogram of electropolymerization confirmed that each electrode facilitate the formation of effective PANI coatings on the surface via well-defined redox cycles. The morphological structures of PANI exhibit well-distributed nanofiber networks on each electrode surface, with slight variations in fiber size and distribution, indicating the ability to obtain conductive PANI coatings with a higher

active surface area, which is essential for fabricating effective supercapacitors. Three heterogeneous symmetric supercapacitors, including PANI-GMMTCE_GKCeCE, PANI-GMMTCeCE_GKCeCE, and PANI-GKCE_GKCeCE constructed using PANI-GKCeCE as one compartment each, and the remaining compartment was utilized among the three, consequently. Each supercapacitor displayed considerably higher specific capacitance based on the cyclic voltammograms and charge-discharge cycles. PANI-GMMTCeCE_GKCeCE and PANI-GMMTCE_GKCeCE achieved higher specific capacitance, while PANI-GKCE_GKCeCE showed comparatively lower specific capacitance from both techniques. All three heterogeneous symmetric supercapacitors are related to a pseudocapacitive nature, based on the CV technique and charge-discharge curves. PANI-GMMTCeCE_GKCeCE displayed comparatively lower R_S and R_{CT} values, confirming well-noticeable characteristics of PANI coatings and PANI-electrode interactions that contribute to a better energy storage process. However, the PANI-GKCE_GKCeCE supercapacitor showcased the lowest R_S among the three of them, proving its synergistic effect to form an effective heterogeneous symmetric supercapacitor by PANI-coated electrodes of GKCeCE and GKCE. Electrochemical impedance circuits demonstrated that all three supercapacitors exhibit both double-layer and pseudocapacitive characteristics with the presence of at least one constant phase element in each circuit. Charge transfer mechanisms of PANI-GMMTCeCE_GKCeCE and PANI-GKCE_GKCeCE supercapacitors followed a conventional ionic diffusion process, similar to previously fabricated graphite-clay-based supercapacitors. PANI-GMMTCE_GKCeCE and PANI-GMMTCeCE_GKCeCE displayed greater energy and power densities compared to PANI-GKCE_GKCeCE, proving that those capabilities in efficient charge transfer and storage as heterogeneous symmetric supercapacitors. Conclusively, all three supercapacitors demonstrated their capabilities in different ways by performing PANI-coated graphite-clay-based heterogeneous symmetric supercapacitors, and further modifications should be implemented to improve the performance of heterogeneous symmetric supercapacitors.

Acknowledgement

This work was financially supported by the Industrial Technology Institute of Sri Lanka (Grant No. TG 24/246).

Conflicts of interest

The authors have no competing interests to declare that are relevant to the content of this article.

References

[1] Gogotsi, Y.; Penner, R. M. Energy storagein nanomaterials-capacitive, pseudocapacitive, or battery-like? *ACS Nano* **2018,** *12*(3), 2081-2083.
[2] Simon, P.; Gogotsi, Y. Materials for electrochemical capacitors. *Nat. Mater.* **2008,** *7*(11), 845-854.
[3] Wang, Q.; Li, J.-L.; Gao, F.; Li, W.-S.; Wu, K.-Z.; Wang, X.-D. Activated carbon coated with polyaniline as an electrode material in supercapacitors. *New Carbon Mater.* **2008,** *23*(3), 275-280.
[4] Zhang, L. L.; Zhao, X. S. Carbon-based materials as supercapacitor electrodes. *Chem. Soc. Rev.* **2009,** *38*(9), 2520-2531.
[5] Arshadi Rastabi, S.; Sarraf-Mamoory, R.; Razaz, G.; Blomquist, N.; Hummelgård, M.; Olin, H. Treatment of $NiMoO_4$/nanographite nanocomposite electrodes using flexible graphite substrate for aqueous hybrid supercapacitors. *PLoS One* **2021,** *16*(7), e0254023.
[6] Arumugam, B.; Mayakrishnan, G.; Subburayan Manickavasagam, S. K.; Kim, S. C.; Vanaraj, R. An overview of active electrode materials for the efficient high-performance supercapacitor application. *Crystals* **2023,** *13*(7), 1118.
[7] Sarkar, S.; Akshaya, R.; Ghosh, S. Nitrogen doped graphene/$CuCr_2O_4$ nanocomposites for supercapacitors application: Effect of nitrogen doping on coulombic efficiency. *Electrochim. Acta* **2020,** *332*, 135368.
[8] Bellido-Milla, D.; Cubillana-Aguilera, L. M.; El Kaoutit, M.; Hernández-Artiga, M. P.; Hidalgo-Hidalgo de Cisneros, J. L.; Naranjo-Rodríguez, I.; Palacios-Santander, J. M. Recent advances in graphite powder-based electrodes. *Anal. Bioanal. Chem.* **2013,** *405*(11), 3525-3539.

[9] Spallacci, C.; Görlin, M.; Kumar, A.; D'Amario, L.; Cheah, M. H. Fabricating high-purity graphite disk electrodes as a cost-effective alternative in fundamental electrochemistry research. *Sci. Rep.* **2024,** *14*(1), 4258.
[10] Karunadasa, K. S. P.; Manoratne, C. H.; Pitawala, H. M. T. G. A.; Rajapakse, R. M. G. A potential working electrode based on graphite and montmorillonite for electrochemical applications in both aqueous and molten salt electrolytes. *Electrochem. Commun.* **2019,** *108*, 106562.
[11] Karunadasa, K. S. P.; Rathnayake, D.; Manoratne, C.; Pitawala, A.; Rajapakse, G. A binder-free composite of graphite and kaolinite as a stable working electrode for general electrochemical applications. *Electrochem. Sci. Adv.* **2021,** *1*(4), e2100003.
[12] Madhushanka, P. M.; Karunadasa, K. S.; Gamage, D., Advancement of graphite-clay composite electrodes via different compositions to improve the synergetic matrix effect towards general electroanalytical and energy storage applications. *Advanced Energy Conversion Materials* **2024,** 5(2), 281-307.
[13] Rathnayake, D. T.; Karunadasa, K. S. P.; Wijekoon, A. S. K.; Manoratne, C. H.; Rajapakse, R. M. G. Low-cost ternary composite of graphite, kaolinite and cement as a potential working electrode for general electrochemical applications. *Chem. Pap.* **2022,** *76*(10), 6653-6658.
[14] Madhushanka, P. M.; Karunadasa, K. S. Graphite composite electrodes for effective charge storage via synergistically improved compositions enriched with kaolinite and cement as matrix inducers. *Adv. Energy Convers. Mater.* **2025,** *6*(1), 83-101.
[15] Rathnayake, D. T.; Karunadasa, K. S. P.; Wijekoon, A. S. K.; Manoratne, C. H.; Gamini Rajapakse, R. M.; Pitawala, H. M. T. G. A. Polyaniline-conjugated graphite-montmorillonite composite electrode prepared by in situ electropolymerization for supercapacitor applications. *Chem. Pap.* **2023,** *77*(5), 2923-2928.
[16] Madhushanka, P. M. H.; Karunadasa, K. S. P.; Gamini Rajapakse, R. M.; Manoratne, C. H.; Bandara, H. M. N. Low-cost composite electrode consisting of graphite, colloidal graphite and montmorillonite with enhanced electrochemical performance for general electroanalytical techniques and device fabrication. *Chem. Pap.* **2024,** *78*(1), 633-643.
[17] Madhushanka, P. M. H.; Karunadasa, K. S. P.; Rajapakse, R. M. G. Graphite-colloidal graphite-kaolinite-cement quaternary composite electrode with improved synergetic matrix effect towards efficient energy storage and electroanalytical applications. *Chem. Pap.* **2024,** *78*, 5585-5598.
[18] Ma, Y.; Hou, C.; Zhang, H.; Qiao, M.; Chen, Y.; Zhang, H.; Zhang, Q.; Guo, Z. Morphology-dependent electrochemical supercapacitors in multi-dimensional polyaniline nanostructures. *J. Mater. Chem. A* **2017,** *5*(27), 14041-14052.
[19] Conway, B. E. *Electrochemical Supercapacitors: Scientific Fundamentals and Technological Applications*; Springer Science & Business Media: New York, 2013.
[20] Mondal, S.; Sangaranarayanan, M. V. Permselectivity and thickness-dependent ion transport properties of overoxidized polyaniline: A mechanistic investigation. *Phys. Chem. Chem. Phys.* **2016,** *18*(44), 30705-30720.
[21] Beygisangchin, M.; Abdul Rashid, S.; Shafie, S.; Sadrolhosseini, A. R.; Lim, H. N. Preparations, properties, and applications of polyaniline and polyaniline thin films-a review. *Polymers* **2021,** *13*(12), 2003.
[22] Beygisangchin, M.; Hossein Baghdadi, A.; Kartom Kamarudin, S.; Abdul Rashid, S.; Jakmunee, J.; Shaari, N. recent progress in polyaniline and its composites: Synthesis, properties, and applications. *Eur. Polym. J.* **2024,** *210*, 112948.
[23] Huerta, F.; Quijada, C.; Montilla, F.; Morallón, E. Revisiting the redox transitions of polyaniline: Semiquantitative interpretation of electrochemically induced IR bands. *J. Electroanal. Chem.* **2021,** *897*, 115593.
[24] Dmitrieva, E.; Dunsch, L. How linear is "linear" polyaniline? *J. Phys. Chem. B* **2011,** *115*(20), 6401-6411.
[25] Gvozdenović, M. M.; Jugović, B. Z.; Stevanović, J. S.; Trišović, T. L.; Grgur, B. N. Electrochemical polymerization of aniline. *Electropolymerization* **2011,** *2011*, 77-96.
[26] Chen, W.; Rakhi, R. B.; Alshareef, H. N. Morphology-dependent enhancement of the pseudocapacitance of template-guided tunable polyaniline nanostructures. *J. Phys. Chem. C* **2013,** *117*(29), 15009-15019.
[27] Park, H.-W.; Kim, T.; Huh, J.; Kang, M.; Lee, J. E.; Yoon, H. Anisotropic growth control of polyaniline nanostructures and their morphology-dependent electrochemical characteristics. *ACS Nano* **2012,** *6*(9), 7624-7633.
[28] Belgherbi, O.; Seid, L.; Lakhdari, D.; Chouder, D.; Akhtar, M. S.; Saeed, M. A. Optical and morphological properties of electropolymerized semiconductor polyaniline thin films: Effect of thickness. *J. Electron. Mater.* **2021,** *50*(7), 3876-3884.
[29] Zhang, H.; Li, H.; Zhang, F.; Wang, J.; Wang, Z.; Wang, S. Polyaniline nanofibers prepared by a facile electrochemical approach and their supercapacitor performance. *J. Mater. Res.* **2008,** *23*(9), 2326-2332.
[30] Zhao, H.-B.; Yuan, L.; Fu, Z.-B.; Wang, C.-Y.; Yang, X.; Zhu, J.-Y.; Qu, J.; Chen, H.-B.; Schiraldi, D. A.

Biomass-based mechanically strong and electrically conductive polymer aerogels and their application for supercapacitors. *ACS Appl. Mater. Interfaces* **2016,** *8*(15), 9917-9924.
[31] Huang, H.; Zeng, X.; Li, W.; Wang, H.; Wang, Q.; Yang, Y. Reinforced conducting hydrogels prepared from the in situ polymerization of aniline in an aqueous solution of sodium alginate. *J. Mater. Chem. A* **2014,** *2*(39), 16516-16522.
[32] Wang, X.; Deng, J.; Duan, X.; Liu, D.; Guo, J.; Liu, P. Crosslinked polyaniline nanorods with improved electrochemical performance as electrode material for supercapacitors. *J. Mater. Chem. A* **2014,** *2*(31), 12323-12329.
[33] Abaspour, M.; Pattipati, K. R.; Shahrrava, B.; Balasingam, B. Robust approach to battery equivalent-circuit-model parameter extraction using electrochemical impedance spectroscopy. *Energies* **2022,** *15*(23), 9251.
[34] Chen, B.-R.; Police, Y. R.; Li, M.; Chinnam, P. R.; Tanim, T. R.; Dufek, E. J. A mathematical approach to survey electrochemical impedance spectroscopy for aging in lithium-ion batteries. *Front. Energy Res.* **2023,** *11*, 167.
[35] Ji, Y.; Schwartz, D. T. Second-harmonic nonlinear electrochemical impedance spectroscopy: Part I. Analytical theory and equivalent circuit representations for planar and porous electrodes. *J. Electrochem. Soc.* **2023,** *170*(12), 123511.
[36] Zhang, J. A.; Wang, P.; Liu, Y.; Cheng, Z. Variable-order equivalent circuit modeling and state of charge estimation of lithium-ion battery based on electrochemical impedance spectroscopy. *Energies* **2021,** *14*(3), 769.
[37] Shanthi, P. M.; Hanumantha, P. J.; Ramalinga, K.; Gattu, B.; Datta, M. K.; Kumta, P. N. Sulfonic acid based complex framework materials (CFM): Nanostructured polysulfide immobilization systems for rechargeable lithium-sulfur Battery. *J. Electrochem. Soc.* **2019,** *166*(10), A1827.
[38] Dubal, D. P.; Lee, S. H.; Kim, J. G.; Kim, W. B.; Lokhande, C. D. Porous polypyrrole clusters prepared by electropolymerization for a high-performance supercapacitor. *J. Mater. Chem.* **2012,** *22*(7), 3044-3052.
[39] Du, H.; Xie, Y.; Xia, C.; Wang, W.; Tian, F. Electrochemical capacitance of polypyrrole-titanium nitride and polypyrrole-titania nanotube hybrids. *New J. Chem.* **2014,** *38*(3), 1284-1293.
[40] Oldenburger, M.; Bedürftig, B.; Gruhle, A.; Grimsmann, F.; Richter, E.; Findeisen, R.; Hintennach, A. Investigation of the low frequency warburg impedance of Li-ion cells by frequency domain measurements. *J. Energy Storage* **2019,** *21*, 272-280.
[41] Huang, J. Diffusion impedance of electroactive materials, electrolytic solutions and porous electrodes: Warburg impedance and beyond. *Electrochim. Acta* **2018,** *281*, 170-188.
[42] Magar, H. S.; Hassan, R. Y. A.; Mulchandani, A. Electrochemical impedance spectroscopy (EIS): Principles, construction, and biosensing applications. *Sensors* **2021,** *21*(19), 6578.
[43] Boratto, M. H.; Lima, J. V. M.; Malliaras, G. G.; Graeff, C. F. O. Supercapacitor auto analyser: An automated data analysis software for supercapacitor characterization. *J. Energy Storage* **2023,** *63*, 107095.
[44] Zheng, Q.; Kvit, A.; Cai, Z.; Ma, Z.; Gong, S. A freestanding cellulose nanofibril-reduced graphene oxide-molybdenum oxynitride aerogel film electrode for all-solid-state supercapacitors with ultrahigh energy density. *J. Mater. Chem. A* **2017,** *5*(24), 12528-12541.
[45] Adnan, S. M.; Zaidi, S. High energy density polyaniline/exfoliated graphite based supercapacitor with improved stability in wide voltage window. *Orient. J. Chem.* **2021,** *37*(2), 450.
[46] Kayode, S. E.; Awobifa, O. S.; Garcia-Lobato, M. A.; Rosas, M. T.; Hoyos, M.; González, F. J. In situ PANI-graphite nanochain-like structures and their application as supercapacitive electrodes. *J. Compos. Sci.* **2024,** *8*(6), 200.
[47] Yesilyurt, E. I.; Pionteck, J.; Simon, F.; Voit, B. Fabrication of PANI/MWCNT supercapacitors based on a chitosan binder and aqueous electrolyte for enhanced energy storage. *RSC Appl. Polym.* **2023,** *1*(1), 97-110.